 doi:10.20944/preprints202203.0225.v1

Article

Doxorubicin-induced Skeletal Muscle Atrophy is Mediated by Mitochondrial Permeability Transition

S. Kyle Travis[1†], Sarah K. Skinner[1†], Trace Thome[2], Liam F. Fitzgerald[1], Michael S. Cohen[3], Dennis W. Wolan[4], Michael J. Toth[5], Terence E. Ryan[2], and Russell T. Hepple[1,6,*]

[1] Department of Physical Therapy, University of Florida, Gainesville, FL 32610, USA
[2] Department of Applied Physiology and Kinesiology, University of Florida, Gainesville, FL, USA
[3] Department of Chemical Physiology and Biochemistry, Oregon Health and Science University, Portland, OR 927239, USA
[4] Departments of Molecular Medicine and Integrative Structural and Computational Biology, Scripps Research, La Jolla, CA 92037, USA
[5] Department of Medicine, University of Burlington, Burlington, VT, USA
[6] Department of Physiology & Functional Genomics, University of Florida, USA
[†] These authors contributed equally
[*] Correspondence: rthepple@ufl.edu; Tel.: +1-352-294-8703 (RTH)

Abstract: Doxorubicin (Dox) is a commonly used chemotherapeutic that can adversely affect skeletal muscle, including causing muscle atrophy. Dox is known to induce an event known as mitochondrial permeability transition (MPT) in cardiac muscle and this plays an important role in Dox-mediated cardiac toxicity. Further to this, recent evidence identifies MPT as a mechanism of atrophy in skeletal muscle, suggesting that MPT may underlie some of the Dox-related toxicity in skeletal muscle. To test this hypothesis, we used cultured human primary myotubes, C2C12 myotubes, and single adult mouse flexor digitorum brevis (FDB) muscle fibers in experiments involving Dox treatment with or without inhibitors of MPT. Dox treatment of myotubes caused myonuclear translocation of the mitochondrial protein apoptosis inducing factor (AIF) and increased mitochondrial reactive oxygen species (mROS), consistent with the known consequences of MPT. Furthermore, Dox caused atrophy in C2C12 myotubes grown on patterned plates, human primary myotubes, and single muscle fibers from adult mice. Notably, Dox-induced atrophy could be prevented by a wide variety of agents that inhibit MPT, as well as by inhibiting mROS or Caspase 3. In conclusion, our results indicate that MPT plays an important role in driving Dox-mediated skeletal muscle atrophy.

Keywords: chemotherapy; muscle atrophy; Doxorubicin; mitochondria; reactive oxygen species

1. Introduction

Skeletal muscle is essential to life and plays an essential role in movement, eating, and breathing. Conditions associated with muscle atrophy, therefore, have far-reaching implications for not only quality of life [1], but if severe can also impact mortality [2]. In this respect, cancer and its treatment can adversely affect skeletal muscle, causing atrophy, impaired contractility and mitochondrial dysfunction [3-8]. These maladaptations are perhaps best characterized in late-stage cancer patients, where both tumor- and treatment-related factors affect muscle [9,10]. However, muscle impairment is also seen in patients with early-stage disease undergoing chemotherapy following tumor removal. For example, breast cancer patients receiving anthracycline-based chemotherapy following tumor resection experience substantial muscle atrophy [11] and weakness [12], underscoring the adverse effects of chemotherapy on skeletal muscle in cancer patients.

To gain insight into the impact of anthracycline-based chemotherapy on skeletal muscle, we previously employed a mouse model of Doxorubicin (Dox)-based chemotherapy [13]. Briefly, chemotherapy treated mice received Dox (*i.p.* 10 mg per kg) on day one of each cycle and Dexamethasone (Dex; *s.c.* 2.5 mg per kg) on days 1 through 5. Dex was

Preprints (www.preprints.org) | NOT PEER-REVIEWED | Posted: 16 March 2022 doi:10.20944/preprints202203.0225.v1

included to emulate clinical regimens, where it prevents anaphylaxis and nausea [14]. Control mice were injected *s.c.* with saline on days 1 through 5. This 5-d chemotherapy treatment was repeated at 3-wk intervals for 4 cycles. Mice were sacrificed 3 months following their 4th cycle of treatment to capture persistent, post-treatment effects of chemotherapy. Dox treated mice exhibited 12% lower gastrocnemius muscle mass versus saline control, and this was accompanied by a 36% lower maximal respiratory capacity and 17% lower citrate synthase enzyme activity in gastrocnemius muscle. Given that impaired physical function is evident in cancer survivors years beyond treatment [15-17], our preclinical data suggest that this is due at least in part to chemotherapy-induced atrophy and persistent mitochondrial respiratory dysfunction in skeletal muscle. This raises the question of the mechanisms by which chemotherapeutic agents affect skeletal muscle, where mounting evidence implicates an important role for mitochondria [18]. Indeed, several previous studies have identified that various chemotherapeutic agents have adverse effects on the mitochondrion in skeletal muscle [19-21], although the consequences of these mitochondrial impacts are poorly understood.

Interestingly, previous studies in human cardiac muscle show that Dox induces an event known as mitochondrial permeability transition (MPT) [22], where MPT is an established mechanism of cardiac toxicity operating through reactive oxygen species (ROS) and activation of the intrinsic pathway of apoptosis (e.g., cytochrome c-mediated increase in Caspase 3 activity) [23]. Although MPT has not been studied directly in skeletal muscle in response to Dox, one study found that Dox-induced toxicity in skeletal muscle required an increase in mROS [24], which is noteworthy because MPT is associated with an increase in mROS release [25]. Furthermore, we recently identified MPT as a novel mechanism of skeletal muscle atrophy that operates through both mROS- and Caspase 3-dependent mechanisms [26]. Building upon this observation, in the present study we conducted experiments involving cultured C2C12 myotubes (a murine muscle cell line), human primary myoblasts, and single isolated muscle fibers from the flexor digitorum longus (FDB) of adult mice to test the hypothesis that Dox-induced skeletal muscle atrophy is mediated through MPT. We also tested the involvement of mROS and caspase 3 activation in this process.

2. Materials and Methods

2.1 Muscle cell culture. C2C12 myoblasts (3-4 biological replicates per experiment) were obtained from ATCC (ATCC Cat # CRL-1772). Myoblasts were cultured in Dulbecco's Modified Eagle's Medium (DMEM: 4.5g/L glucose, 110 mg/L sodium pyruvate, and 2mM GlutaMax) supplemented with 10% FBS and 1% penicillin/streptomycin. In some experiments, C2C12 myoblasts were differentiated on micromolded/patterned hydrogels to promote greater maturation as previously described [27]. Human primary myoblasts were isolated from four donors (age = 58 ± 8 y, 3 male/1 female) that underwent a muscle biopsy procedure. All human study procedures were approved by the institutional review board at the University of Florida (Protocol 201801553) and carried out according to the Declaration of Helsinki. Participants were fully informed about the research and provided written informed consent. The isolation procedures and culturing methods of human primary myoblasts have been previously described [28-30]. Myoblast differentiation was initiated by serum withdrawal using DMEM (4.5g/L glucose, 110 mg/L sodium pyruvate, and 2mM GlutaMax) supplemented with 2% heat-inactivated horse serum and 1% penicillin/streptomycin. Differentiation medium was changed every 24 hours until experimentation. All cells were cultured in standard conditions at 37°C and 5% CO_2.

2.2 MPT and Nuclear Translocation of AIF. C2C12 myotubes were treated with 1μM Dox (Sigma D1515) or vehicle (phosphate buffered saline; PBS) beginning at day 4 of differentiation to induce MPT. To modulate MPT in response to Dox, cells treated with Dox were also treated with either 1μM Cyclosporin A (CsA; Sigma C1832), 1μM bongkrekic acid (BA) (Sigma B6179), 5μM mitoTEMPO (Sigma SML0737), 25μM Morin

Preprints (www.preprints.org) | NOT PEER-REVIEWED | Posted: 16 March 2022 doi:10.20944/preprints202203.0225.v1

hydrate (Morin; Sigma M4008), 0.5μM Isoxazole 63 (Isox63), or vehicle (DMSO – all equal volume) at the same time as the addition of Dox. After 48 h of treatment, myotubes were washed twice with PBS and fixed with 4% paraformaldehyde for 10 min. Cells were permeabilized with PBS + 0.2% triton X-100 for 10 min with gentle shaking, then blocked with PBS + 5% goat serum + 1% bovine serum albumin (BSA) for one hour at room temperature. Cells were incubated with primary antibody against apoptosis inducing factor (AIF; Abcam ab32516) at 1:300 in blocking solution overnight at 4°C. Cells were then washed 3x in PBS, followed by incubation with 1:500 secondary antibody (AlexaFluor594, mouse IgG2b, ThermoFisher) for one hour at 37°C. Cells were washed 3x in PBS, incubated with DAPI stain (Nucblue, ThermoFisher) and then imaged using automated capture routines on an Evos FL Auto 2 inverted fluorescent microscope (ThermoFisher). Five 20x images were captured per well (n=4-5 wells per group) and analyzed by calculating a Mander's coefficient for colocalization between the AIF and DAPI signals, indicating AIF translocation to the nucleus. All processing procedures were performed uniformly over the entire set of images by a blinded investigator using ImageJ plugin Coloc2.

2.3 Myotube Mitochondrial Oxidative Stress. C2C12 or human primary myotubes were treated with 1μM Dox (Sigma D1515) or vehicle (PBS) beginning at day 4 of differentiation to induce MPT. As above, cells treated with Dox were also treated with either 1μM CsA (Sigma C1832) to inhibit MPT, 1μM BA (Sigma B6179) to inhibit MPT, or 5μM mitoTEMPO (Sigma SML0737) to scavenge mROS, at the same time of addition of Dox. To account for the impact of MPT on mROS production and how this related to myotube atrophy, after 24 hours of treatment, myotubes were washed twice with Hanks balanced salt solution (HBSS) and incubated with 500nM MitoSox (ThermoFisher) for 15 min in HBSS prior to imaging. Sixteen 20x images were captured per well (N=4-5 wells per group) and analyzed using custom written routines in CellProfiler (Broad Institute) to assess both mitoSox positive area and mean intensity. All processing procedures were performed uniformly over the entire set of images using batch processing modes to remove any human bias.

2.4 Myotube Atrophy. Myotubes were treated with 1μM Dox (Sigma D1515) or vehicle (PBS) beginning at day 4 of differentiation to induce MPT. To examine the role of MPT in myotube atrophy, cells treated with Dox were also treated with either 1μM CsA (Sigma C1832), 1μM bongkrekic acid (BA) (Sigma B6179), 5μM mitoTEMPO (Sigma SML0737), 25μM morin hydrate (Sigma M4008), 0.5μM Isox63, or vehicle (DMSO – all equal volume) at the same time of addition of Dox. After 48 hours of treatment, myotubes were washed twice with PBS and fixed/permeabilized with ice cold methanol/acetone (1:1) for 10 min. Cells were then blocked with PBS + 5% goat serum + 1% BSA for one hour at room temperature. Cells were incubated with primary antibody against sarcomeric myosin (MF 20 was deposited to the Developmental Studies Hybridoma Bank by Fischman, D.A. (DSHB Hybridoma Product MF 20)) at 1:25 in blocking solution for one hour at 37°C. Cells were then washed 3x in PBS, followed by incubation with 1:250 secondary antibody (AlexaFluor594, mouse IgG2b, ThermoFisher) for one hour at 37°C. Cells were washed 3x in PBS, then imaged using automated capture routines on an Evos FL Auto 2 inverted fluorescent microscope. Sixty-four 20x images were captured per well (N=4 biological replicates per group) and analyzed using custom written routines in CellProfiler (Broad Institute) to assess MF20+ area (myotube area). All processing procedures were performed uniformly over the entire set of images using batch processing modes to remove any human input.

2.5 *shRNA Experiments Targeting Caspase 3.* pLKO.1 puro was a gift from Bob Weinberg (Addgene plasmid # 8453) [31]. The shRNA cloning cassette from pLKO.1 puro was PCR amplified and inserted into a promoterless AAV cloning vector (Cellbiolabs) using In-Fusion cloning (Takara). The resultant pAAV-LKO.1 puro plasmid was linearized with AgeI and EcoRI and purified by gel extraction. To knockdown Caspase 3,

Preprints (www.preprints.org) | NOT PEER-REVIEWED | Posted: 16 March 2022 doi:10.20944/preprints202203.0225.v1

a shRNA sequence for mouse CASP3 was obtained from Millipore-Sigma Mission shRNA library TRCN0000321020. The shRNA duplex was inserted in the linearized pAAV-LKO.1 puro plasmid via a ligation reaction. The resulting plasmids were transfected into C2C12 muscle cells at day 4 of differentiation using Xfect reagent (Takara), and myotubes were subsequently treated with 1μM Dox 48 hours later. A nonsense scrambled shRNA sequence was used as a negative control.

2.6 Animals and Surgical Methods for Single FDB muscle fiber isolation. All procedures were conducted with approval from the University of Florida Institutional Animal Care and Use Committee (protocol #202011171, to R.T. Hepple). Male C57BL/6 mice were housed in ventilated cages, and provided food and water *ad libitum*. On the day of sacrifice, mice were anesthetized with 2-4% isoflurane. FDBs were carefully dissected and removed from both hindlimbs, trimmed of excess fat, blood vessels, and surrounding connective tissue in room-temperature physiological rodent saline (PRS: 138 mM NaCl, 2.7 mM KCl, 1.8 mM $CaCl_2$, 1.06 mM $MgCl_2$, 12.4 mM HEPES and 5.6 mM glucose, pH 7.3). Following isolation of the muscles, mice were killed by thoracotomy and removal of the heart.

2.7 Single Muscle Fiber Isolation and Culture. FDB muscles were prepared for single muscle fiber isolation according to previously established methods [32,33]. Immediately after isolation, both FDB muscles from a given mouse were incubated in an Eppendorf tube containing a solution of 1.5 mL PRS with 0.2% collagenase type I (Worthington, USA), 0.1% elastase (Worthington), 0.0625% protease from *Streptomyces griseus* (Sigma-Aldrich, USA), 0.033% dispase (Invitrogen, USA), and 10% fetal bovine serum (FBS, Invitrogen) and maintained at 37°C and 5% CO_2 for 95 min to digest the inter-muscle fiber connective tissue. After digestion, muscles were moved to a 35 mm culture dish containing proliferative medium (PM: high-glucose Dulbecco's modified Eagle's medium (DMEM, Life Technologies, USA) containing 10% FBS, 1% antibiotic-antimycotic mix (Life Technologies), and 0.1% gentamycin (Life Technologies) and incubated for 5 min. Whole muscles were then triturated with warm proliferative medium using a P1000 pipette for dissociation into single muscle fibers. Individual muscle fibers were transferred to 35 mm culture dishes (n=100-150 fibers) containing maintenance media (MM: high-glucose DMEM supplemented with 20% 1X Serum Replacement 2; Sigma-Aldrich) and kept under standard culture conditions for the duration of the experiment.

2.8 Dox Treatment in Adult Mouse Single FDB Muscle Fiber Culture. To confirm if Dox induces atrophy through MPT in single muscle fibers from mouse FDB muscle (as seen in C2C12 and human primary myotubes), we first treated single FDB muscle fibers from one male mouse with (i) vehicle (water), (ii) 1 μM Dox, or (iii) 1 μM Dox and 1 μM of the MPT inhibitor CsA (as in myotube cultures above) for 24 h. Based upon our previous observations showing that MPT-induced atrophy required an increase in mROS and caspase 3 activity [33], we then conducted a second series of single FDB muscle fiber experiments to determine if Dox-mediated atrophy also required mROS and caspase 3. Specifically, single FDB muscle fibers from 3 male mice were treated with (i) vehicle (ddH_2O), (ii) 1 μM Dox, (iii) 1 μM Dox and 0.5 μM of the MPT inhibitor Isox63; (iv) 1 μM Dox and 5 μM of the mROS scavenger MitoTEMPO (as in myotube experiments); or (v) 1 μM Dox and 20 μM of the novel caspase 3 inhibitor Ac-AT010-KE.

All muscle fibers were subsequently imaged by brightfield illumination on a customized Leica SP8 microscope (Leica Microsystems, Wetzlar, Germany) following plating to permit baseline measurements of myofiber diameter, and imaged again following 24 h incubation in the conditions noted above. Culture dishes were placed in a pre-warmed stage-top incubator (Tokai Hit, Shizuoka, Japan) at 37°C, and tiled images were taken of the entire dish. Images were stitched and exported for analysis in ImageJ. Single fibers were numbered and a total of 50 single fibers were selected at random for the analysis. Measurements were collected along the length of each fiber to capture proximal, proximal-medial, medial, distal-medial, and distal diameters. Fiber diameters were then

 doi:10.20944/preprints202203.0225.v1

averaged to provide a mean fiber diameter value per each selected fiber. Fibers that were visually hypercontracted were excluded from the analysis, as described previously [33].

Statistics

Statistical comparisons between treatments employed a nested ANOVA to take account of both technical replicates and biological replicates within each experimental group/condition. Individual group differences were identified with a Sidak post-hoc test. The *p*-value for determining significance was set at <0.05.

3. Results

3.1. Dox Treatment in Skeletal Muscle Myotubes

We first tested whether Dox induces MPT in skeletal muscle cells. Consistent with the established effects of MPT in other tissues, C2C12 myotubes treated with 1 μM Dox for 24 h exhibited a marked increase in myonuclear AIF levels (Fig 1). Notably, the myonuclear translocation of AIF following Dox treatment was attenuated by two different MPT inhibitors that act through distinct mechanisms: CsA, which inhibits the MPT-regulating protein cyclophilin D (CypD); and Bonkrekic Acid (BA), which inhibits the adenine nucleotide transporter (ANT). Furthermore, Dox-induced myonuclear AIF translocation could also be prevented by blocking mROS with MitoTempo. As MPT in other tissues is associated with an increase in mROS, we also sought to determine if Dox induced an increase in mROS in skeletal muscle in a manner that depends upon MPT. Consistent with this notion, C2C12 myotubes treated with 1 μM Dox for 24 h exhibited an increased area of staining for the mROS-sensitive probe MitoSox (Fig 2), and as with myonuclear translocation of AIF, this was also attenuated both by inhibiting MPT (CsA, BA) or by scavening mROS using mitoTEMPO.

Preprints (www.preprints.org) | NOT PEER-REVIEWED | Posted: 16 March 2022 doi:10.20944/preprints202203.0225.v1

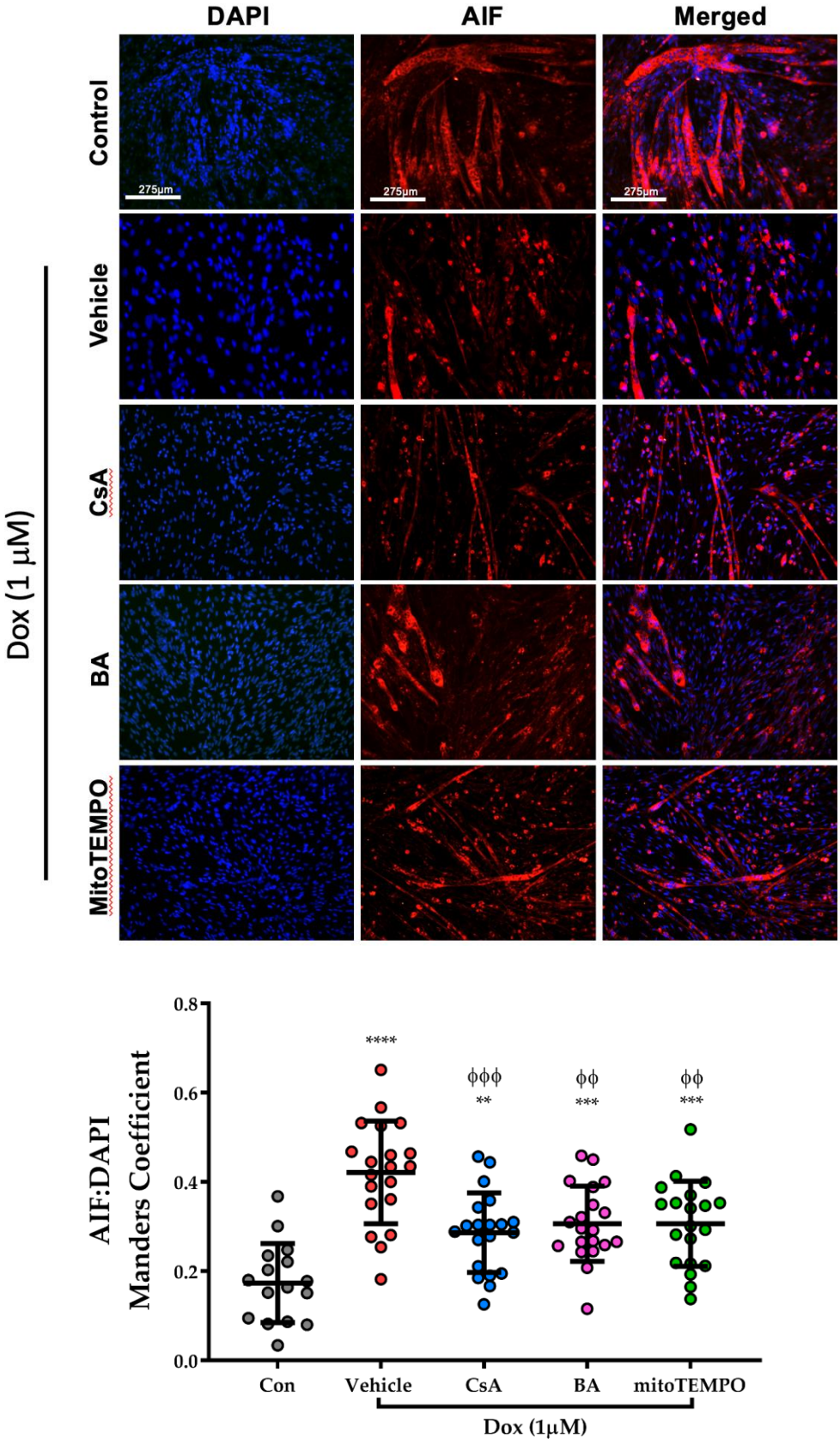

Figure 1. *Treatment of C2C12 myotubes with Dox for 48 h causes nuclear translocation of the mitochondrial protein, AIF (apoptosis inducing factor), and this is prevented by MPT inhibitors*

Preprints (www.preprints.org) | NOT PEER-REVIEWED | Posted: 16 March 2022 doi:10.20944/preprints202203.0225.v1

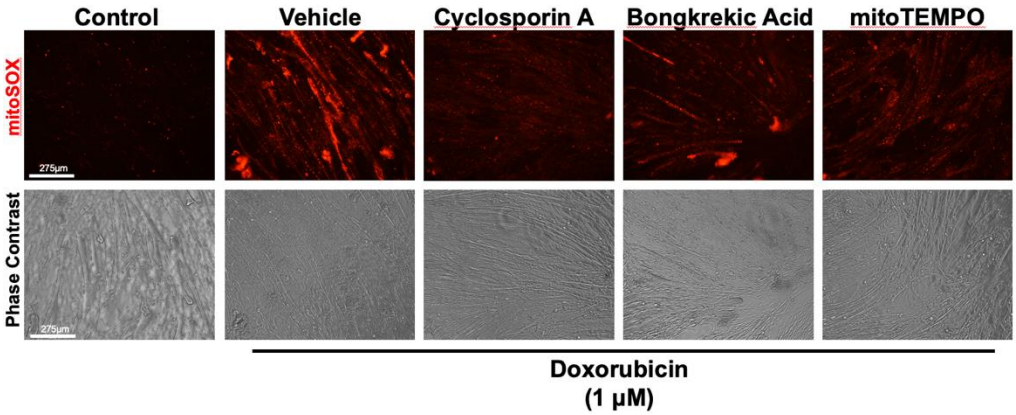

(CsA [Cyclosporin A], BA [Bonkrekic Acd]) or by scavening mROS (mitoTEMPO). ****p<0.0001 versus Con. $^{\phi}p$<0.01, $^{\phi}p$<0.001 versus Vehicle.

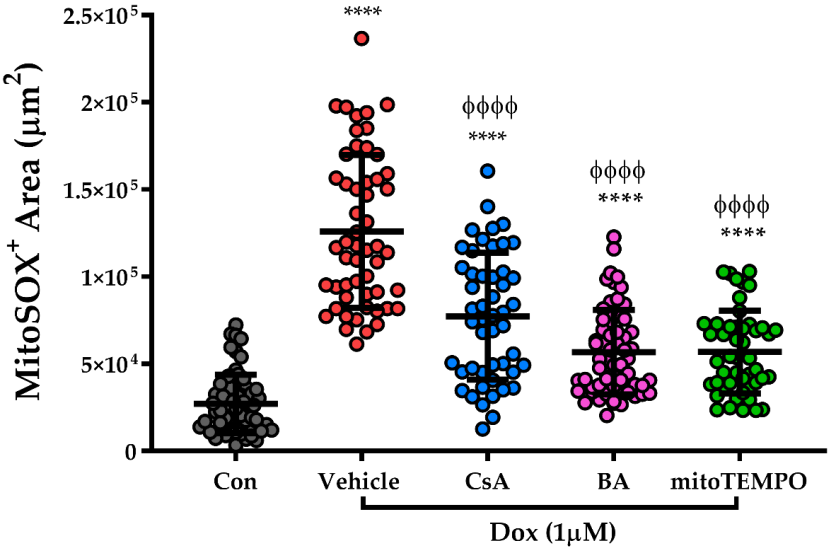

Figure 2. *Treatment of C2C12 myotubes with Dox for 48 h caused an increase in the positive area of MitoSox fluorescence, consistent with an increase in mROS. This was attenuated by inhibitors of MPT (CsA [Cyclosporin A], BA [Bonkrekic Acid]) or by scavening mROS with mitoTEMPO.* ***p<0.001, ****p<0.0001 versus Con. $^{\phi}p$<0.0001 versus Vehicle.

3.2. Dox Treatment Causes Skeletal Muscle Atrophy

To evaluate the role of MPT in mediating skeletal muscle atrophy following exposure to Dox, we first performed studies in C2C12 myotubes seeded on patterned plates. 24 h following Dox treatment there was significant myotube atrophy that was attenuated by the MPT inhibitor CsA (Fig. 3). We then confirmed these findings in human primary myotubes from 4 human donors, where Dox also induced atrophy that was prevented by a variety of MPT inhibitors that operate through distinct mechanisms (CsA, BA, Morin, and isox63) (Fig. 4). Finally, we treated single adult mouse FDB muscle fibers with Dox, where Dox-induced atrophy could also be prevented by MPT inhibition (Fig.

Preprints (www.preprints.org) | NOT PEER-REVIEWED | Posted: 16 March 2022 doi:10.20944/preprints202203.0225.v1

5). Thus, our results are consistent in showing that Dox induces atrophy of skeletal muscle in a manner that depends upon MPT.

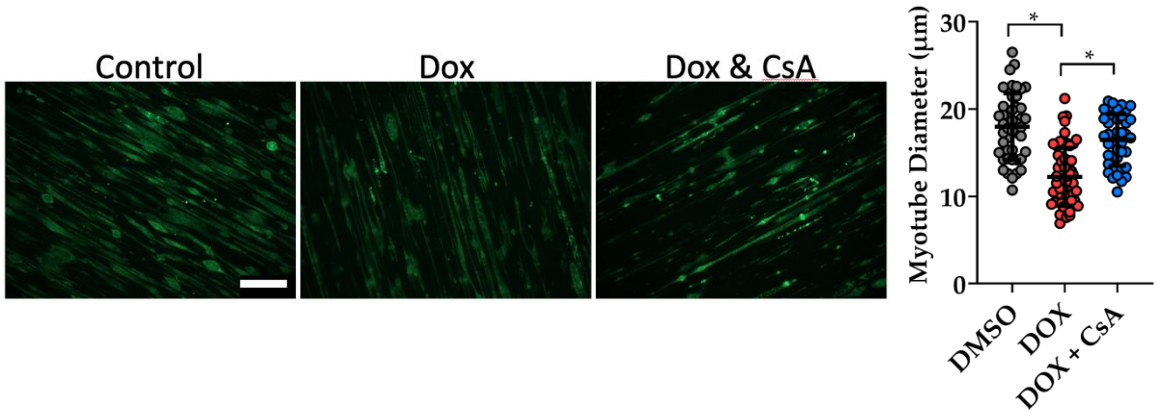

Figure 3. *C2C12 myotubes grown on a patterned plate and treated with Dox for 48 h exhibited atrophy that was prevented by treatment with the MPT inhibitor CsA (Cyclosporin A). Bar = 300 µm. *p<0.05 versus Dox.*

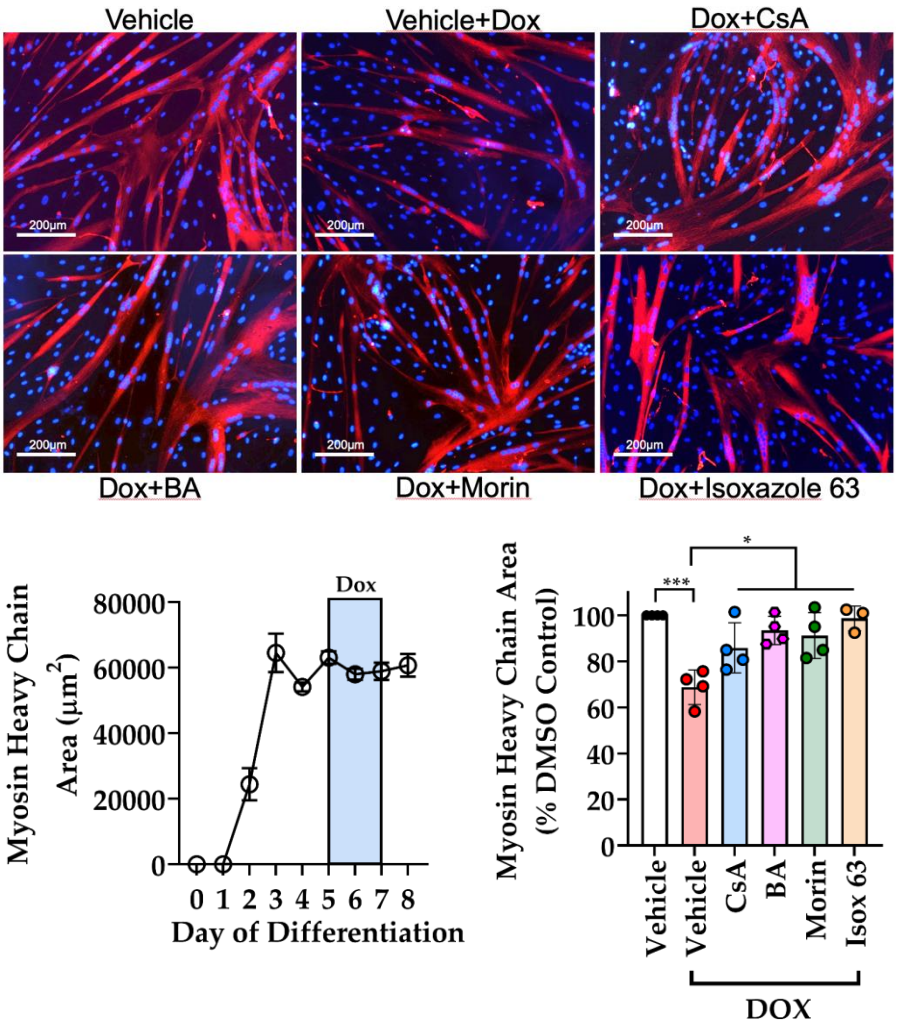

Figure 4. *Treatment of human primary myotubes with Dox for 48 h caused atrophy that was prevented by a variety of MPT inhibitors (CsA [Cyclosporin A], BA [Bonkrekic Acid], the phytochemical Morin, Isox63).*

Preprints (www.preprints.org) | NOT PEER-REVIEWED | Posted: 16 March 2022 doi:10.20944/preprints202203.0225.v1

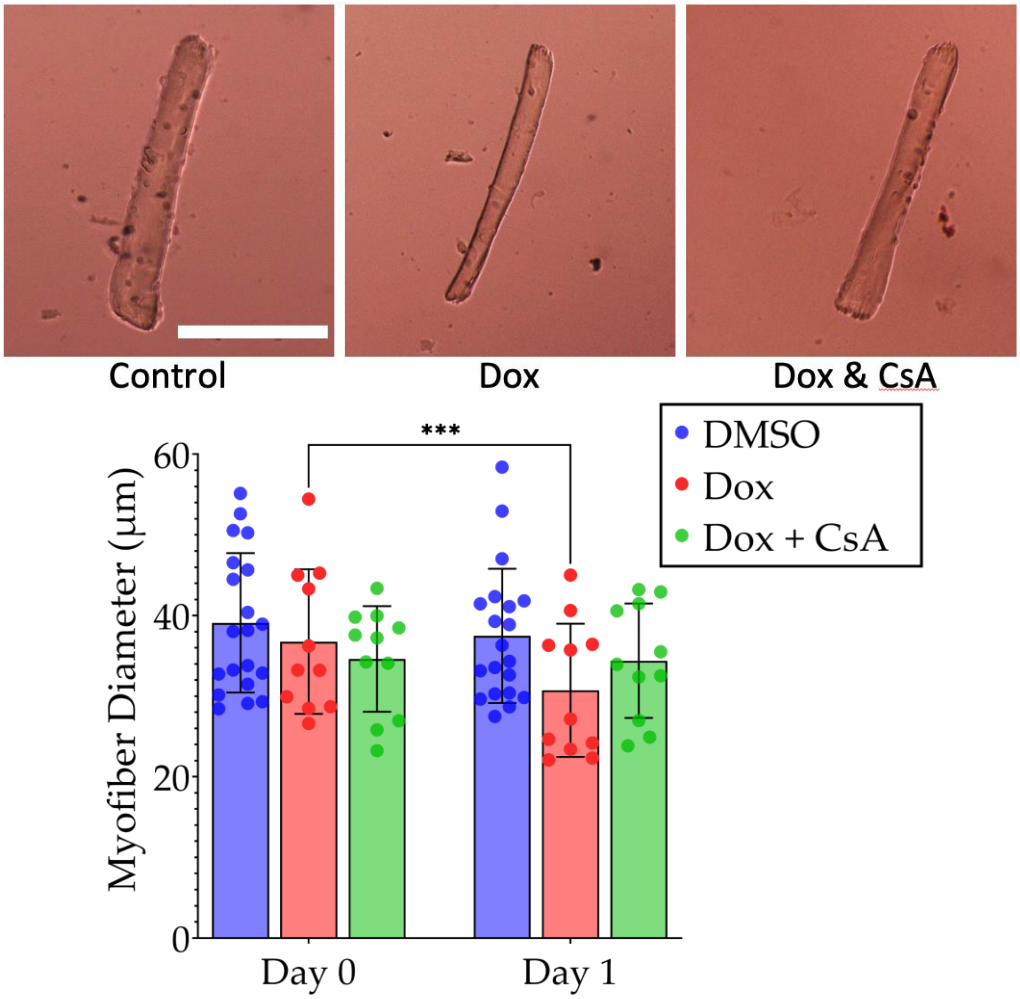

Figure 5. *Treatment of mouse single FDB muscle fibers with Dox for 24 h caused muscle fiber atrophy that was prevented by the MPT inhibitor, CsA (Cyclosporin A). Bar = 200 μm. ***p<0.0005.*

3.3. Dox-induced Skeletal Muscle Atrophy Requires mROS and Caspase 3

To assess the roles of mROS and Caspase 3 in Dox-induced MPT causing muscle atrophy, we first tested the impact of scavenging mROS using MitoTEMPO in Dox-induced atrophy in C2C12 myotubes, finding that MitoTEMPO prevented Dox-induced atrophy similarly to the MPT inhibitors CsA and BA (Fig. 6). We then utilized an shRNA targeting Caspase 3, which caused an approximately 60% reduction in Caspase 3 RNA expression, and found that knockdown of Caspase 3 also prevented Dox-induced atrophy in C2C12 myotubes (Fig 7). To translate these findings in myoblast culture to adult muscle, we then confirmed these findings in single FDB muscle fibers from 3 adult mice, finding that blocking mROS with MitoTempo or blocking Caspase 3 activity using the selective Caspase 3 inhibitor Ac-ATS010-KE [34] prevented Dox-induced muscle fiber atrophy in a manner that was quantitatively similar to the atrophy protection conferred by the MPT inhibitor Isox63 (Fig 8). Thus, collectively, our results indicate that Dox-induced MPT causes muscle atrophy that depends upon both mROS and caspase 3 activation.

Preprints (www.preprints.org) | NOT PEER-REVIEWED | Posted: 16 March 2022 doi:10.20944/preprints202203.0225.v1

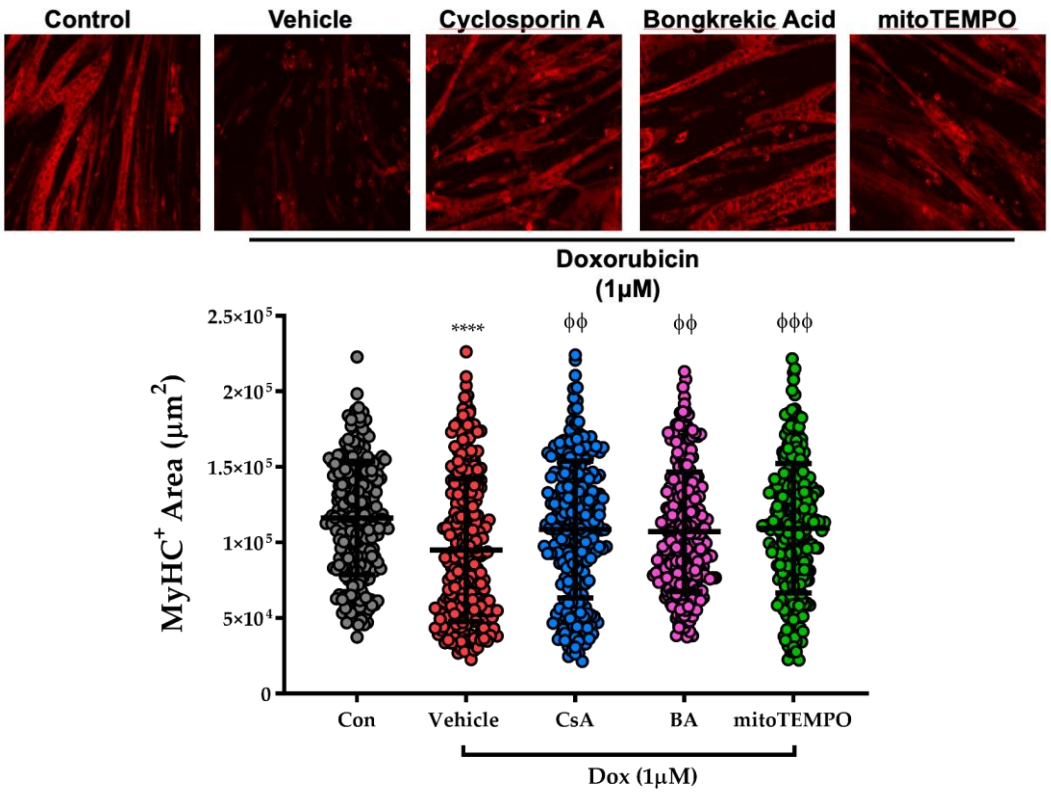

Figure 6. The reduction in size of C2C12 myotubes after treatment with Dox for 48 h was prevented by quenching mROS (mitoTEMPO).

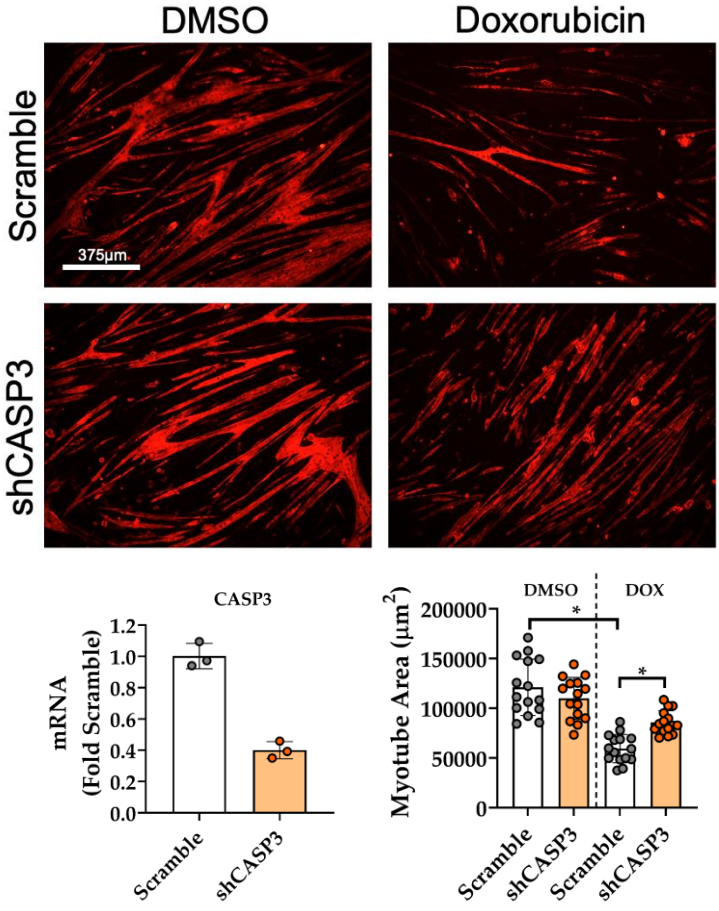

Figure 7. The reduction in C2C12 myotube size following 48 h treatment with Dox was largely abolished following transfection of shRNA targeting Caspase 3 (CASP3). *P<0.05.

Preprints (www.preprints.org) | NOT PEER-REVIEWED | Posted: 16 March 2022 doi:10.20944/preprints202203.0225.v1

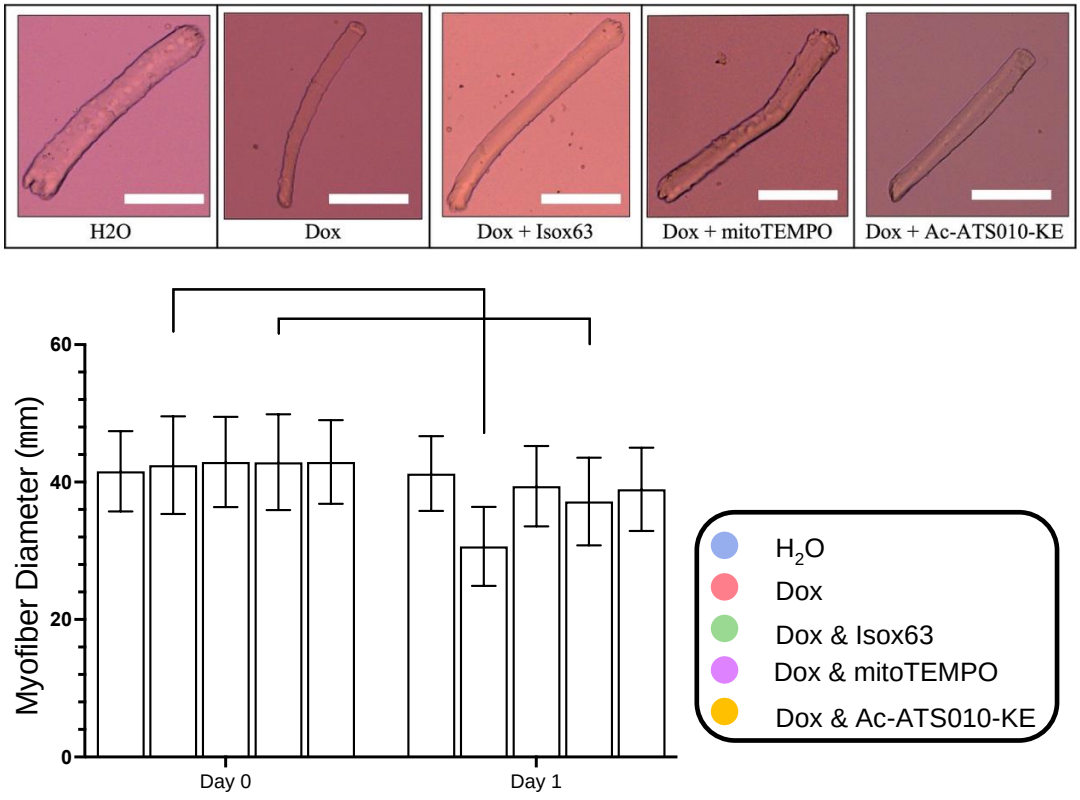

Figure 8. The atrophy of single FDB muscle fibers from adult mice following 24 h treatment with Dox was prevented by inhibiting MPT (Isox63), or by scavenging mROS (mitoTEMPO) or inhibiting Caspase 3 activity (Ac-ATS010-KE). Bar = 200 μm. *p<0.05, **p<0.01.

4. Discussion

There is growing understanding that various chemotherapeutic agents used in treating cancers can have deleterious impacts on skeletal muscle, independent of the tumor. These agents include the anthracycline, Dox, where previous studies have revealed that cancer patients undergoing Dox chemotherapy can exhibit muscle atrophy [11] and weakness [12]. Furthermore, preclinical studies in mice have shown that the adverse effects of Dox treatment on skeletal muscle can persist for several months following cessation of treatment [13], consistent with long-term physical impairment in cancer survivors [35] , which diminishes quality of life. These findings underscore the need for greater understanding of the mechanisms responsible for Dox-induced muscle impairment. Skeletal muscle mitochondria are impacted by various chemotherapeutic agents [18], including Dox [13], and studies in heart find that Dox induces an event known as mitochondrial permeability transition (MPT) [22] that in turn causes an increase in mROS production and initiation of proteolytic/apoptotic signaling such as increased activity of Caspase 3 [36]. Based upon our recent evidence showing that MPT in skeletal muscle induces atrophy in a manner that depends upon an increase in mROS and Caspase 3 activity [26], the purpose of the current study was to test the hypothesis that Dox-induced muscle atrophy is mediated by MPT. To test this hypothesis, we used a series of cell and tissue culture approaches including C2C12 myotubes, human primary myotubes, and single muscle fibers from adult mice maintained in culture, in combination with genetic and pharmacological manipulations to alter MPT and its downstream effectors. Our data show that Dox induces myonuclear translocation of the mitochondrial protein AIF and increases mROS, consistent with the established effects of MPT in other tissues [37,38]. Furthermore, we observed that Dox caused muscle atrophy in C2C12 myotubes, human primary myotubes, and single mouse muscle fibers that was inhibited by a wide variety of MPT inhibitors operating through distinct mechanisms from one another. Finally, our data show that

Preprints (www.preprints.org) | NOT PEER-REVIEWED | Posted: 16 March 2022 doi:10.20944/preprints202203.0225.v1

Dox-induced muscle atrophy requires both mROS and Caspase 3, based upon results of experiments involving quenching of mROS using the mitochondrial-targeted antioxidant mitoTempo in C2C12 myotubes and single mouse muscle fibers, and experiments employing either genetic knockdown of Caspase 3 by shRNA in C2C12 myotubes or chemical inhibition of Caspase 3 activity in single mouse muscle fibers using the novel inhibitor Ac-ATS010-KE. Collectively, therefore, our results show that Dox induces skeletal muscle atrophy in a manner that depends upon MPT, and which requires mROS and activation of Caspase 3. Importantly, these discoveries implicate MPT as a potential therapeutic target for reducing the adverse impact of Dox chemotherapy on skeletal muscle.

Dox-induced MPT in Skeletal Muscle. MPT is a well-known mechanism of cytotoxicity, particularly in the context of ischemic organ injury [39-41]. Although the molecular identity of the structure(s) responsible for MPT pore formation remains intensely studied [42], the fundamental events that constitute MPT have been known for several decades. Generally, MPT events may be categorized as those that are brief with low conductance to help dissipate excess mitochondrial membrane potential [43] and regulate mitochondrial Ca^{2+} signaling [44], and those that are prolonged with high conductance leading to oxidative stress and cell death. Although low conductance MPT events may be necessary for normal function of the cell, the high conductance toxic form of MPT is implicated in an increasingly diverse array of pathological settings in various tissues [36], including Dox-induced cardiac toxicity [45]. We know comparatively less about the functions or consequences of MPT in skeletal muscle than other tissues, although skeletal muscle mitochondria have been known to undergo MPT in aging [46] and in some pathologies of muscle such as muscular dystrophy [47]. However, we recently identified MPT as a novel mechanism causing skeletal muscle atrophy through mechanisms that require mROS and Caspase 3 activation [26]. Although Dox has well-established toxicity in skeletal muscle [13,48,49], whether it requires MPT has not been established, despite MPT being an established Dox-induced cytotoxic mechanism in cardiac muscle [22,45].

Previous studies have observed alterations in skeletal muscle following Dox treatment that hint at the possible involvement of MPT, such as an increase in mROS [13,20,24,50]. To test whether Dox induces MPT in skeletal muscle we treated C2C12 myotubes with Dox for 48 h and subsequently fixed and labeled the myotubes to permit us to examine the amount of the mitochondrial protein AIF that translocated to the myonuclei. The basis for this assay is that MPT permits the release of a variety of mitochondrial-localized proteins, some of which (e.g., AIF) target the nucleus to initiate degradation of DNA as part of the cell death pathway [38]. Hence, the degree to which Dox induces an increase in myonuclear AIF can be used as a readout for the occurrence of MPT. Consistent with the impact of Dox in causing MPT in the heart [22], our experiments show that Dox induced a marked increase in the abundance of myonuclei that labelled positively for AIF. This was prevented by two MPT inhibitors that operate through distinct mechanisms (i.e., CsA which inhibits the mitochondrial protein cyclophilin D to raise the threshold for MPT [51]; BA which inhibits the adenine nucleotide transporter [52], one of the putative components of the MPT pore [53]). Therefore, our results are consistent with Dox causing MPT in skeletal muscle. Since there is also an increase in mROS release during MPT [26,37], we then determined whether Dox caused an increase in mROS emission using the mROS-sensitive probe, mitoSox. Our results show that Dox induced a significant increase in the area of tissue that is positive for mitoSox fluorescence. The attenuation of the Dox-induced increase in mitoSox positive area by MPT inhibitors indicates that a significant fraction of the Dox-induced increase in mROS is secondary to the impact of Dox on MPT.

Dox, MPT and Skeletal Muscle Atrophy. As noted above, our recent work identifies MPT as a mechanism causing skeletal muscle atrophy [26]. Furthermore, our results discussed above show that, like the impact of Dox in causing MPT in heart [22], Dox also induces MPT in skeletal muscle. Therefore, to directly test the involvement of MPT in Dox-mediated muscle atrophy, we first determined whether Dox would induce atrophy of

C2C12 myotubes grown on patterned plates. Consistent with Dox mediating muscle atrophy through MPT-dependent mechanisms, our results showed that Dox treatment of C2C12 myotubes for 48 h induced atrophy that could be prevented by the MPT inhibitor CsA. To assess whether this also occurred in human skeletal muscle, we then treated human primary myotubes with Dox and observed significant atrophy that was prevented by a wide variety of MPT inhibitors acting through distinct mechanisms. These inhibitors include the aforementioned CsA and BA, as well the phytochemical Morin which likely has pleiotropic effects on mitochondria in preventing MPT [54], and isox63 which is a newly developed compound that acts through CypD-independent mechanisms [55]. We then extended our findings to single skeletal muscle fibers from adult mouse and also observed that Dox induced atrophy in a manner that required MPT. As such, our data provide clear evidence that Dox induces skeletal muscle atrophy and can be prevented by inhibiting/reducing MPT.

To help understand the mechanisms by which Dox-mediated MPT causes atrophy, we then conducted experiments in C2C12 myotubes involving chemical inhibition of mROS using mitoTEMPO, and both genetic (shRNA) and chemical inhibition of Caspase 3. The rationale for focusing on mROS and Caspase 3 is based upon extensive literature implicating mROS in various muscle atrophy conditions [56-60], and a somewhat lesser body of evidence for the involvement of Caspase 3 in muscle atrophy [61-63]. Moreover, we have recently confirmed that, as in other tissues [36], MPT in skeletal muscle induces an increase in mROS and Caspase 3 activity [26]. Consistent with our previous observations concerning the mechanisms by which MPT induces atrophy in skeletal muscle, the myotube atrophy resulting from Dox-induced MPT was prevented by scavening mROS and by both genetic and chemical approaches for blocking Caspase 3 in C2C12 myotubes. We then confirmed these results in single adult muscle fibers, finding that scavenging mROS and Caspase 3 inhibition prevented the atrophy occurring with Dox-induced MPT in single mouse FDB muscle fibers. Collectively, therefore, our results show that Dox induces skeletal muscle atrophy and that this requires MPT and its downstream sequelae, mROS and Caspase 3 activation. The significance of these findings is that they provide insights to some of the mechanisms that are likely to underlie the adverse effects of Dox on skeletal muscle. On the other hand, much remains to be understood concerning the mechanisms involved in MPT-induced muscle atrophy. This includes determining whether myonuclear translocation of AIF is also associated with nuclear DNA degradation. Furthermore, it will also be important to identify the mechanisms by which Dox is causing MPT in skeletal muscle, noting that Dox causes cellular disruptions that have been identified as triggers for MPT [40], such as marked Ca^{2+} dyshomeostasis and ROS-mediated oxidative stress [64]. Finally, in view of the mitochondrial impairment seen with a variety of chemotherapeutic agents [65], many of which have established skeletal muscle impact [18], it will also be valuable to address the potential role of MPT in chemotherapy-induced skeletal muscle impairment more broadly.

Author Contributions: Conceptualization: RTH, TER, MJT; Materials and Technical Support: SKT, SKB, LF, TT, MFC, DWW, and TER; Data acquisition & analysis: TT, SKT, LF and SKB; Manuscript Original Draft: RTH. All authors have read and agreed to the final version of the manuscript.

Funding: This research was supported by the National Institutes of Health National Institute on Aging (R56 AG066758 to RTH), a University of Florida Opportunity Seed Fund (to RTH), and the National Institutes of Health National Institute of General Medical Sciences (R35 GM136286 to DWW). SKB was supported by a Predoctoral Training Fellowship on a T32 grant from the National Institute of Health National Institute of Child Health and Human Development (T32 HD043730). TT was supported by a Ruth L. Kirschstein National Research Service Award Fellowship from the National Institutes of Health National Institute of Diabetes Digestive Health and Kidney Disease (F31-DK128920). LFF was supported by an American Heart Association Postdoctoral Fellowship (POST836216).

Institutional Review Board Statement: Human study procedures (muscle biopsy) were approved by the institutional review board at the University of Florida (Protocol 201801553 to TER) and

carried out according to the Declaration of Helsinki and participants were fully informed about the research and informed consent was obtained. All procedures involving mice were conducted with approval from the University of Florida Institutional Animal Care and Use Committee (Protocol #202011171 to RTH).

Informed Consent Statement: Informed consent was obtained from the human participants who donated primary myoblasts for this study.

Data Availability Statement: In this section, please provide details regarding where data supporting reported results can be found, including links to publicly archived datasets analyzed or generated during the study. Please refer to suggested Data Availability Statements in section "MDPI Research Data Policies" at https://www.mdpi.com/ethics. If the study did not report any data, you might add "Not applicable" here.

Acknowledgments: The authors acknowledge the help of Dr. Karyn Esser's lab, particularly her Postdoctoral Trainees Dr. Denise Kemler and Dr. Christopher Wolff, for their assistance in setting up the approach that involved C2C12 myotube culture on patterned plates.

Conflicts of Interest: The authors declare no conflict of interest. The funders had no role in the design of the study; in the collection, analyses, or interpretation of data; in the writing of the manuscript, or in the decision to publish the results.

References

1. Hanna, L.; Nguo, K.; Furness, K.; Porter, J.; Huggins, C.E. Association between skeletal muscle mass and quality of life in adults with cancer: a systematic review and meta-analysis. *Journal of cachexia, sarcopenia and muscle* **2022**, doi:10.1002/jcsm.12928.
2. Liu, M.; Zhang, Z.; Zhou, C.; Ye, Z.; He, P.; Zhang, Y.; Li, H.; Liu, C.; Qin, X. Predicted fat mass and lean mass in relation to all-cause and cause-specific mortality. *Journal of cachexia, sarcopenia and muscle* **2022**, doi:10.1002/jcsm.12921.
3. Toth, M.J.; Miller, M.S.; Callahan, D.M.; Sweeny, A.P.; Nunez, I.; Grunberg, S.M.; Der-Torossian, H.; Couch, M.E.; Dittus, K. Molecular mechanisms underlying skeletal muscle weakness in human cancer: reduced myosin-actin cross-bridge formation and kinetics. *J Appl Physiol* **2013**, *114*, 858-868, doi:10.1152/japplphysiol.01474.2012.
4. Tisdale, M. Mechanisms of cancer cachexia. *Physiol Rev* **2009**, *89*, 381 - 410.
5. White, J.P.; Baltgalvis, K.A.; Puppa, M.J.; Sato, S.; Baynes, J.W.; Carson, J.A. Muscle oxidative capacity during IL-6-dependent cancer cachexia. *Am J Physiol* **2011**, *300*, R201-R211, doi:10.1152/ajpregu.00300.2010.
6. Fermoselle, C.; García-Arumí, E.; Puig-Vilanova, E.; Andreu, A.L.; Urtreger, A.J.; de Kier Joffé, E.D.B.; Tejedor, A.; Puente-Maestu, L.; Barreiro, E. Mitochondrial dysfunction and therapeutic approaches in respiratory and limb muscles of cancer cachectic mice. *Exp Physiol* **2013**, *98*, 1349-1365, doi:10.1113/expphysiol.2013.072496.
7. Julienne, C.; Dumas, J.-F.; Goupille, C.; Pinault, M.; Berri, C.; Collin, A.; Tesseraud, S.; Couet, C.; Servais, S. Cancer cachexia is associated with a decrease in skeletal muscle mitochondrial oxidative capacities without alteration of ATP production efficiency. *J Cachexia Sarcopenia Muscle* **2012**, *3*, 265-275, doi:10.1007/s13539-012-0071-9.
8. Tzika, A.A.; Fontes-Oliveria, C.C.; Shestova, A.A.; Constantinou, C.; Psychogios, N.; Righi, V.; Mintzopoulos, D.; Busquets, S.; Lopez-Soriano, F.J.; Milote, S.; et al. Skeletal muscle mitochondrial uncoupling in a murine cancer cachexia model. *Int J Oncol* **2013**, *43*, 886-894.
9. Biswas, A.K.; Acharyya, S. Understanding cachexia in the context of metastatic progression. *Nat Rev Cancer* **2020**, *20*, 274-284, doi:10.1038/s41568-020-0251-4.
10. Barreto, R.; Mandili, G.; Witzmann, F.A.; Novelli, F.; Zimmers, T.A.; Bonetto, A. Cancer and Chemotherapy Contribute to Muscle Loss by Activating Common Signaling Pathways. *Front Physiol* **2016**, *7*, 472, doi:10.3389/fphys.2016.00472.

11. Freedman, R.J.; Aziz, N.; Albanes, D.; Hartman, T.; Danforth, D.; Hill, S.; Sebring, N.; Reynolds, J.C.; Yanovski, J.A. Weight and body composition changes during and after adjuvant chemotherapy in women with breast cancer. *J Clin Endocrinol Metab* **2004**, *89*, 2248-2253, doi:doi:10.1210/jc.2003-031874.
12. Klassen, O.; Schmidt, M.E.; Ulrich, C.M.; Schneeweiss, A.; Potthoff, K.; Steindorf, K.; Wiskemann, J. Muscle strength in breast cancer patients receiving different treatment regimes. *J Cachexia Sarcopenia Muscle* **2016**, *8*, 305-316, doi:10.1002/jcsm.12165.
13. Gouspillou, G.; Scheede-Bergdahl, C.; Spendiff, S.; Vuda, M.; Meehan, B.; Mlynarski, H.; Archer-Lahlou, E.; Sgarioto, N.; Purves-Smith, F.M.; Konokhova, Y.; et al. Anthracycline-containing chemotherapy causes long-term impairment of mitochondrial respiration and increased reactive oxygen species release in skeletal muscle. *Scientific reports* **2015**, *5*, 8717, doi:10.1038/srep08717.
14. Guigni, B.A.; Callahan, D.M.; Tourville, T.W.; Miller, M.S.; Fiske, B.R.; Voigt, T.B.; Korwin-Mihavics, B.; Anathy, V.; Dittus, K.; Toth, M.J. Skeletal muscle atrophy and dysfunction in breast cancer patients: role for chemotherapy-derived oxidant stress. *Am J Physiol Cell Physiol* **2018**, *315*, C744-C756, doi:10.1152/ajpcell.00002.2018.
15. Lakoski, S.G.; Barlow, C.E.; Koelwyn, G.J.; Hornsby, W.E.; Hernandez, J.; DeFina, L.F.; Radford, N.B.; Thomas, S.M.; Herndon, J.E., II; Peppercorn, J.; et al. The influence of adjuvant therapy on cardiorespiratory fitness in early-stage breast cancer seven years after diagnosis: the Cooper Center Longitudinal Study. *Breast Cancer Res Treat* **2013**, *138*, 909-916, doi:10.1007/s10549-013-2478-1.
16. Peel, A.B.; Barlow, C.E.; Leonard, D.; DeFina, L.F.; Jones, L.W.; Lakoski, S.G. Cardiorespiratory fitness in survivors of cervical, endometrial, and ovarian cancers: The Cooper Center Longitudinal Study. *Gynecologic oncology* **2015**, *138*, 394-397, doi:10.1016/j.ygyno.2015.05.027.
17. Jones, L.W.; Courneya, K.S.; Mackey, J.R.; Muss, H.B.; Pituskin, E.N.; Scott, J.M.; Hornsby, W.E.; Coan, A.D.; Herndon, J.E.; Douglas, P.S.; et al. Cardiopulmonary function and age-related decline across the breast cancer survivorship continuum. *J Clin Oncol* **2012**, *30*, 2530-2537, doi:10.1200/jco.2011.39.9014.
18. Sorensen, J.C.; Cheregi, B.D.; Timpani, C.A.; Nurgali, K.; Hayes, A.; Rybalka, E. Mitochondria: Inadvertent targets in chemotherapy-induced skeletal muscle toxicity and wasting? *Cancer Chemother Pharmacol* **2016**, doi:10.1007/s00280-016-3045-3.
19. Barreto, R.; Waning, D.L.; Gao, H.; Liu, Y.; Zimmers, T.A.; Bonetto, A. Chemotherapy-related cachexia is associated with mitochondrial depletion and the activation of ERK1/2 and p38 MAPKs. *Oncotarget* **2016**, doi:10.18632/oncotarget.9779.
20. Gilliam, L.A.; Fisher-Wellman, K.H.; Lin, C.T.; Maples, J.M.; Cathey, B.L.; Neufer, P.D. The anticancer agent doxorubicin disrupts mitochondrial energy metabolism and redox balance in skeletal muscle. *Free Radic Biol Med* **2013**, *65*, 988-996, doi:10.1016/j.freeradbiomed.2013.08.191.
21. Ramos, S.V.; Hughes, M.C.; Perry, C.G.R. Altered skeletal muscle microtubule-mitochondrial VDAC2 binding is related to bioenergetic impairments after paclitaxel but not vinblastine chemotherapies. *Am J Physiol Cell Physiol* **2019**, *316*, C449-C455, doi:10.1152/ajpcell.00384.2018.
22. Montaigne, D.; Marechal, X.; Preau, S.; Baccouch, R.; Modine, T.; Fayad, G.; Lancel, S.; Neviere, R. Doxorubicin induces mitochondrial permeability transition and contractile dysfunction in the human myocardium. *Mitochondrion* **2011**, *11*, 22-26, doi:10.1016/j.mito.2010.06.001.
23. Kwong, J.Q.; Molkentin, J.D. Physiological and pathological roles of the mitochondrial permeability transition pore in the heart. *Cell Metab* **2015**, *21*, 206-214, doi:10.1016/j.cmet.2014.12.001.
24. Min, K.; Kwon, O.S.; Smuder, A.J.; Wiggs, M.P.; Sollanek, K.J.; Christou, D.D.; Yoo, J.K.; Hwang, M.H.; Szeto, H.H.; Kavazis, A.N.; et al. Increased mitochondrial emission of reactive oxygen species and calpain activation are required for doxorubicin-induced cardiac and skeletal muscle myopathy. *J Physiol* **2015**, *593*, 2017-2036, doi:10.1113/jphysiol.2014.286518.

25. Batandier, C.; Leverve, X.; Fontaine, E. Opening of the mitochondrial permeability transition pore induces reactive oxygen species production at the level of the respiratory chain complex I. *J Biol Chem* **2004**, *279*, 17197-17204, doi:10.1074/jbc.M310329200.
26. Burke, S.K.; Solania, A.; Wolan, D.W.; Cohen, M.S.; Ryan, T.E.; Hepple, R.T. Mitochondrial permeability transition causes mitochondrial reative oxygen species- and caspase 3-dependent atrophy of single adult mouse skeletal muscle fibers. *Cells* **2021**, *10*, 2586, doi:10.3390/cells10102586.
27. Denes, L.T.; Riley, L.A.; Mijares, J.R.; Arboleda, J.D.; McKee, K.; Esser, K.A.; Wang, E.T. Culturing C2C12 myotubes on micromolded gelatin hydrogels accelerates myotube maturation. *Skeletal Muscle* **2019**, *9*.
28. Ryan, T.E.; Yamaguchi, D.J.; Schmidt, C.A.; Zeczycki, T.N.; Shaikh, S.R.; Brophy, P.; Green, T.D.; Tarpey, M.D.; Karnekar, R.; Goldberg, E.J.; et al. Extensive skeletal muscle cell mitochondriopathy distinguishes critical limb ischemia patients from claudicants. *JCI Insight* **2018**, *3*, doi:10.1172/jci.insight.123235.
29. Ryan, T.E.; Schmidt, C.A.; Tarpey, M.D.; Amorese, A.J.; Yamaguchi, D.J.; Goldberg, E.J.; Inigo, M.M.R.; Karnekar, R.; O'Rourke, A.; Ervasti, J.M.; et al. PFKFB3-mediated glycolysis rescues myopathic outcomes in the ischemic limb. *Jci Insight* **2020**, *5*, doi:ARTN e139628
10.1172/jci.insight.139628.
30. Heden, T.D.; Ryan, T.E.; Ferrara, P.J.; Hickner, R.C.; Brophy, P.M.; Neufer, P.D.; McClung, J.M.; Funai, K. Greater Oxidative Capacity in Primary Myotubes from Endurance-trained Women. *Med Sci Sports Exerc* **2017**, *49*, 2151-2157, doi:10.1249/MSS.0000000000001352.
31. Stewart, S.A.; Dykxhoorn, D.M.; Palliser, D.; Mizuno, H.; Yu, E.Y.; An, D.S.; Sabatini, D.M.; Chen, I.S.; Hahn, W.C.; Sharp, P.A.; et al. Lentivirus-delivered stable gene silencing by RNAi in primary cells. *RNA* **2003**, *9*, 493-501, doi:10.1261/rna.2192803.
32. Komiya, Y.; Anderson, J.E.; Akahoshi, M.; Nakamura, M.; Tatsumi, R.; Ikeuchi, Y.; Mizunoya, W. Protocol for rat single muscle fiber isolation and culture. *Anal Biochem* **2015**, *482*, 22-24, doi:10.1016/j.ab.2015.03.034.
33. Burke, S.K.; Solania, A.; Wolan, D.W.; Cohen, M.S.; Ryan, T.E.; Hepple, R.T. Mitochondrial Permeability Transition Causes Mitochondrial Reactive Oxygen Species- and Caspase 3-Dependent Atrophy of Single Adult Mouse Skeletal Muscle Fibers. *Cells* **2021**, *10*, doi:10.3390/cells10102586.
34. Solania, A.; Gonzalez-Paez, G.E.; Wolan, D.W. Selective and Rapid Cell-Permeable Inhibitor of Human Caspase-3. *ACS Chem Biol* **2019**, *14*, 2463-2470, doi:10.1021/acschembio.9b00564.
35. Scheede-Bergdahl, C.; Jagoe, R.T. After the chemotherapy: potential mechanisms for chemotherapy-induced delayed skeletal muscle dysfunction in survivors of acute lymphoblastic leukaemia in childhood. *Front Pharmacol* **2013**, *4*, 49, doi:10.3389/fphar.2013.00049.
36. Bernardi, P.; Rasola, A.; Forte, M.; Lippe, G. The Mitochondrial Permeability Transition Pore: Channel Formation by F-ATP Synthase, Integration in Signal Transduction, and Role in Pathophysiology. *Physiol Rev* **2015**, *95*, 1111-1155, doi:10.1152/physrev.00001.2015.
37. Akopova, O.V.; Kolchynskayia, L.Y.; Nosar, V.Y.; Smyrnov, A.N.; Malisheva, M.K.; Man'kovskaia, Y.N.; Sahach, V.F. The effect of permeability transition pore opening on reactive oxygen species production in rat brain mitochondria. *Ukr Biokhim Zh (1999)* **2011**, *83*, 46-55.
38. Susin, S.A.; Lorenzo, H.K.; Zamzami, N.; Marzo, I.; Snow, B.E.; Brothers, G.M.; Mangion, J.; Jacotot, E.; Costantini, P.; Loeffler, M.; et al. Molecular characterization of mitochondrial apoptosis-inducing factor. *Nature* **1999**, *397*, 441-446, doi:10.1038/17135.
39. Di Lisa, F.; Menabo, R.; Canton, M.; Barile, M.; Bernardi, P. Opening of the mitochondrial permeability transition pore causes depletion of mitochondrial and cytosolic NAD+ and is a causative event in the death of myocytes in postischemic reperfusion of the heart. *J Biol Chem* **2001**, *276*, 2571-2575, doi:10.1074/jbc.M006825200.

40. Lemasters, J.J.; Theruvath, T.P.; Zhong, Z.; Nieminen, A.L. Mitochondrial calcium and the permeability transition in cell death. *Biochim Biophys Acta* **2009**, *1787*, 1395-1401, doi:10.1016/j.bbabio.2009.06.009.
41. Bonora, M.; Patergnani, S.; Ramaccini, D.; Morciano, G.; Pedriali, G.; Kahsay, A.E.; Bouhamida, E.; Giorgi, C.; Wieckowski, M.R.; Pinton, P. Physiopathology of the Permeability Transition Pore: Molecular Mechanisms in Human Pathology. *Biomolecules* **2020**, *10*, doi:10.3390/biom10070998.
42. Bernardi, P.; Carraro, M.; Lippe, G. The mitochondrial permeability transition: Recent progress and open questions. *FEBS J* **2021**, doi:10.1111/febs.16254.
43. Feng, G.; Liu, B.; Li, J.; Cheng, T.; Huang, Z.; Wang, X.; Cheng, H.P. Mitoflash biogenesis and its role in the autoregulation of mitochondrial proton electrochemical potential. *J Gen Physiol* **2019**, doi:10.1085/jgp.201812176.
44. Mnatsakanyan, N.; Beutner, G.; Porter, G.A.; Alavian, K.N.; Jonas, E.A. Physiological roles of the mitochondrial permeability transition pore. *Journal of bioenergetics and biomembranes* **2016**, doi:10.1007/s10863-016-9652-1.
45. Wallace, K.B.; Sardao, V.A.; Oliveira, P.J. Mitochondrial Determinants of Doxorubicin-Induced Cardiomyopathy. *Circ Res* **2020**, *126*, 926-941, doi:10.1161/CIRCRESAHA.119.314681.
46. Gouspillou, G.; Sgarioto, N.; Kapchinsky, S.; Purves-Smith, F.; Norris, B.; Pion, C.H.; Barbat-Artigas, S.; Lemieux, F.; Taivassalo, T.; Morais, J.A.; et al. Increased sensitivity to mitochondrial permeability transition and myonuclear translocation of endonuclease G in atrophied muscle of physically active older humans. *FASEB J* **2014**, *28*, 1621-1633, doi:10.1096/fj.13-242750.
47. Dubinin, M.V.; Talanov, E.Y.; Tenkov, K.S.; Starinets, V.S.; Mikheeva, I.B.; Sharapov, M.G.; Belosludtsev, K.N. Duchenne muscular dystrophy is associated with the inhibition of calcium uniport in mitochondria and an increased sensitivity of the organelles to the calcium-induced permeability transition. *Biochim Biophys Acta Mol Basis Dis* **2020**, *1866*, 165674, doi:10.1016/j.bbadis.2020.165674.
48. Gilliam, L.A.; Ferreira, L.F.; Bruton, J.D.; Moylan, J.S.; Westerblad, H.; St Clair, D.K.; Reid, M.B. Doxorubicin acts through tumor necrosis factor receptor subtype 1 to cause dysfunction of murine skeletal muscle. *J Appl Physiol* **2009**, *107*, 1935-1942, doi:00776.2009 [pii]
10.1152/japplphysiol.00776.2009.
49. Gilliam, L.A.; Moylan, J.S.; Callahan, L.A.; Sumandea, M.P.; Reid, M.B. Doxorubicin causes diaphragm weakness in murine models of cancer chemotherapy. *Muscle Nerve* **2011**, *43*, 94-102, doi:10.1002/mus.21809.
50. Gilliam, L.A.; Moylan, J.S.; Patterson, E.W.; Smith, J.D.; Wilson, A.S.; Rabbani, Z.; Reid, M.B. Doxorubicin acts via mitochondrial ROS to stimulate catabolism in C2C12 myotubes. *Am J Physiol Cell Physiol* **2012**, *302*, C195-202, doi:10.1152/ajpcell.00217.2011.
51. Di Lisa, F.; Bernardi, P. A CaPful of mechanisms regulating the mitochondrial permeability transition. *J Mol Cell Cardiol* **2009**, *46*, 775-780, doi:10.1016/j.yjmcc.2009.03.006.
52. Anwar, M.; Kasper, A.; Steck, A.R.; Schier, J.G. Bongkrekic Acid-a Review of a Lesser-Known Mitochondrial Toxin. *J Med Toxicol* **2017**, *13*, 173-179, doi:10.1007/s13181-016-0577-1.
53. Karch, J.; Bround, M.J.; Khalil, H.; Sargent, M.A.; Latchman, N.; Terada, N.; Peixoto, P.M.; Molkentin, J.D. Inhibition of mitochondrial permeability transition by deletion of the ANT family and CypD. *Sci Adv* **2019**, *5*, eaaw4597, doi:10.1126/sciadv.aaw4597.
54. Liu, S.; Wu, N.; Miao, J.; Huang, Z.; Li, X.; Jia, P.; Guo, Y.; Jia, D. Protective effect of morin on myocardial ischemiareperfusion injury in rats. *Int J Mol Med* **2018**, *42*, 1379-1390, doi:10.3892/ijmm.2018.3743.
55. Antonucci, S.; Di Sante, M.; Sileikyte, J.; Deveraux, J.; Bauer, T.; Bround, M.J.; Menabo, R.; Paillard, M.; Alanova, P.; Carraro, M.; et al. A novel class of cardioprotective small-molecule PTP inhibitors. *Pharmacol Res* **2019**, *151*, 104548, doi:10.1016/j.phrs.2019.104548.

56. Powers, S.K.; Morton, A.B.; Ahn, B.; Smuder, A.J. Redox control of skeletal muscle atrophy. *Free Radic Biol Med* **2016**, *98*, 208-217, doi:10.1016/j.freeradbiomed.2016.02.021.

57. Min, K.; Smuder, A.J.; Kwon, O.S.; Kavazis, A.N.; Szeto, H.H.; Powers, S.K. Mitochondrial-targeted antioxidants protect the skeletal muscle against immobilization-induced muscle atrophy. *Journal of applied physiology* **2011**, doi:10.1152/japplphysiol.00591.2011.

58. Powers, S.K.; Hudson, M.B.; Nelson, W.B.; Talbert, E.E.; Min, K.; Szeto, H.H.; Kavazis, A.N.; Smuder, A.J. Mitochondria-targeted antioxidants protect against mechanical ventilation-induced diaphragm weakness. *Crit Care Med* **2011**, *39*, 1749-1759, doi:10.1097/CCM.0b013e3182190b62.

59. Muller, F.L.; Song, W.; Jang, Y.C.; Liu, Y.; Sabia, M.; Richardson, A.; Van Remmen, H. Denervation-induced skeletal muscle atrophy is associated with increased mitochondrial ROS production. *Am J Physiol Regul Integr Comp Physiol* **2007**, *293*, R1159-1168, doi:00767.2006 [pii]

10.1152/ajpregu.00767.2006.

60. Dodd, S.L.; Gagnon, B.J.; Senf, S.M.; Hain, B.A.; Judge, A.R. Ros-mediated activation of NF-kappaB and Foxo during muscle disuse. *Muscle Nerve* **2010**, *41*, 110-113, doi:10.1002/mus.21526.

61. Du, J.; Wang, X.; Miereles, C.; Bailey, J.L.; Debigare, R.; Zheng, B.; Price, S.R.; Mitch, W.E. Activation of caspase-3 is an initial step triggering accelerated muscle proteolysis in catabolic conditions. *J Clin Invest* **2004**, *113*, 115-123, doi:10.1172/JCI18330.

62. Wang, X.H.; Zhang, L.; Mitch, W.E.; LeDoux, J.M.; Hu, J.; Du, J. Caspase-3 cleaves specific 19 S proteasome subunits in skeletal muscle stimulating proteasome activity. *J Biol Chem* **2010**, *285*, 21249-21257, doi:10.1074/jbc.M109.041707.

63. Silva, K.A.; Dong, J.; Dong, Y.; Dong, Y.; Schor, N.; Tweardy, D.J.; Zhang, L.; Mitch, W.E. Inhibition of Stat3 activation suppresses caspase-3 and the ubiquitin-proteasome system, leading to preservation of muscle mass in cancer cachexia. *J Biol Chem* **2015**, *290*, 11177-11187, doi:10.1074/jbc.M115.641514.

64. Kuznetsov, A.V.; Margreiter, R.; Amberger, A.; Saks, V.; Grimm, M. Changes in mitochondrial redox state, membrane potential and calcium precede mitochondrial dysfunction in doxorubicin-induced cell death. *Biochim Biophys Acta* **2011**, *1813*, 1144-1152, doi:10.1016/j.bbamcr.2011.03.002.

65. Sarosiek, K.A.; Ni Chonghaile, T.; Letai, A. Mitochondria: gatekeepers of response to chemotherapy. *Trends Cell Biol* **2013**, *23*, 612-619, doi:10.1016/j.tcb.2013.08.003.

1.